

Photoproduction of π^- on ^{14}N

V. DeCarlo, N. Freed, and W. Rhodes

Department of Physics, The Pennsylvania State University, 104 Davey Laboratory, University Park, Pennsylvania 16802

B. Bülow, G. G. Jonsson, K. Lindgren, and R. Pettersson

Department of Nuclear Physics, University of Lund, Sölvegatan 14, S-223 62 Lund, Sweden

(Received 10 October 1978; revised manuscript received 17 December 1979)

The reaction $^{14}\text{N}(\gamma, \pi^-)^{14}\text{O}_{\text{g.s.}}$ is calculated within the framework of the distorted wave impulse approximation and the results compared to activation measurements. Investigations are made of the energy dependence of the pion momentum dependent terms in the single particle amplitude and the effects of the nuclear wave function and pion optical potential on total cross sections.

[NUCLEAR REACTION $^{14}\text{N}(\gamma, \pi^-)^{14}\text{O}$. Activation method. $E_0=150-700$ MeV; measured σ_a , deduced σ_b ; calculated σ_b . Ge(Li) detector.]

The levels $^{14}\text{C}(\text{g.s.})$, $^{14}\text{N}(2.31 \text{ MeV})$, and $^{14}\text{O}(\text{g.s.})$ form an isotriplet which connects to the $^{14}\text{N}(\text{g.s.})$ isosinglet via β^+ and $M1$ transitions. It has long been known¹ that the reaction $^{14}\text{C} \rightarrow ^{14}\text{N} + e^- + \bar{\nu}_e$ is anomalously slow. Although the angular momentum, parities, and i spins are consistent with an allowed Gamow-Teller (GT) transition, the large ft value (corresponding to a GT matrix element $|\langle \text{GT} \rangle| = 0.002$) implies, for low momentum transfer, a weak overlap of the ^{14}C and ^{14}N ground states with respect to the axial vector current operator. More recently,² the ^{14}O positron decay to $^{14}\text{N}(\text{g.s.})$ was found also to be strongly inhibited ($|\langle \text{GT} \rangle| = 0.013$) with an ft value approximately 10^4 times greater than that for allowed $0^+ \rightarrow 1^+$ transitions.

In the soft-pion limit,³ radiative pion capture and threshold pion photoproduction, as well as allowed muon capture, are governed by matrix elements similar to that of GT β decay. Within the past few years, studies⁴⁻⁶ of these processes have been carried out on ^{14}N and indicate that at the much higher values of momentum transfer characteristic of these reactions, weak overlaps persist between isotriplet and isosinglet members of the $A=14$ isobars. Although the existence of higher-order contributions (two-body terms, exchange currents, etc.) to the single particle Kroll-Ruderman term in both β decay and photoproduction, together with the higher momentum transfers being sampled in the latter, rule out any immediate comparison between the two processes, it will be nevertheless instructive to use these isobars to investigate the energy dependence of those additional terms in the production amplitude which are dependent on pion momentum and ignored in such allowed transitions as occur^{7,8} at

threshold in $A=6$ and 12 . It will also be interesting to observe the effect of the pion wave function in modifying the results expected on the basis of a pure GT operator.

In this paper we confine our attention to the reaction $^{14}\text{N}(\gamma, \pi^-)^{14}\text{O}$. This reaction proceeds entirely to the ^{14}O ground state which is the only bound state. We also investigate, from the threshold region through the Δ resonance, the dependence of the results on nuclear wave functions and on the optical potentials used to describe the π -nucleus final state interactions. Finally, we present results of activation measurements taken at the Lund synchrotron and compare experimental data with theory.

The calculations are carried out in the framework of the distorted-wave impulse approximation (DWIA) with final state interactions included through optical potentials. Although the theory has been outlined earlier in some detail,^{9,10} it is worthwhile to elaborate here on some additional points specific to this reaction. The free $\gamma\pi N$ amplitude is written in the π -nucleon c.m. system¹¹

$$t = [i\vec{\sigma} \cdot \vec{\epsilon} F_1 + (\vec{\sigma} \cdot \hat{k})\vec{\sigma} \cdot (\hat{K} \times \vec{\epsilon}) F_2 + i(\vec{\sigma} \cdot \hat{K})(\hat{k} \cdot \vec{\epsilon}) F_3 + i(\vec{\sigma} \cdot \hat{k})(\hat{k} \cdot \vec{\epsilon}) F_4] \tau^+ \quad (1)$$

where $\vec{\sigma}$ and $\vec{\epsilon}$ are the nucleon spin and photon polarization, τ^+ is an isospin operator, and \hat{k} and \hat{K} are unit vectors in the direction of pion and photon c.m. momenta. The amplitude factors F_i for $\gamma n \rightarrow \pi^- p$ are decomposed into multipoles in the usual way.¹¹ The individual multipole contributions for $l_\pi \leq 3$ are taken from the work of Berends *et al.*,¹² for photon energies $E_\gamma \geq 160$ MeV and from Weaver¹³ for $E_\gamma = 150$ MeV [Weaver's

results are too high by a factor of $(1 + m_\pi/m_n)^2$; the correct Kroll-Ruderman $m_\pi \rightarrow 0$ prediction is $17.7 \mu\text{b}$ and not $23.1 \mu\text{b}$ as quoted in Ref. 13. The correct values are used here.] Our use of Weaver's result is, in a sense, equivalent to the approach of Ref. 8 in which a renormalization of the dipole strength served to incorporate the linear corrections (in m_π) to the Kroll-Ruderman result for (γ, π^-) .

Three sets of nuclear wave functions were used. The first is the (8-16) *2BME* version of Cohen and Kurath¹⁴ (CK) with a $p_{3/2} - p_{1/2}$ energy splitting of 5.67 MeV. These wave functions give good fits to a wide range of electromagnetic properties in the p shell and in addition predict the cancellation in the $^{14}\text{C} - ^{14}\text{N}$ GT matrix element. The second set arises from the realistic interaction calculation of Lee,¹⁵ as applied by Baer *et al.*,⁴ to radiative π capture on ^{14}N . These wave functions result in a somewhat poorer cancellation in the β -decay matrix element but yield good results for π capture and electron scattering in the p shell. Finally, for comparison purposes only, we use *jj*-coupling wave functions which reproduce very poorly almost all properties in the upper p shell. Harmonic oscillator wave functions are used throughout with an oscillator length $b = 1.70 \text{ fm}$ ($\hbar\omega = 14.35 \text{ MeV}$). We have investigated the influence of *sd*-shell admixtures to the ^{14}O and ^{14}N ground states, using as a guide the weak-coupling calculations of Lie.¹⁶ We find the changes in cross section to be negligible, consistent with the result¹⁶ that the two states contain at most 5% (*sd*)² admixtures.

The final calculational ingredient is the π -nucleus optical potential. It is well known that pion photoproduction is sensitive to the details of the π -nucleus interaction, and it is to be hoped that this sensitivity will eventually be useful in delineating the form of V_{opt} . For the present, we will employ the optical potential of Stricker, McManus, and Carr (SMC),¹⁷ which has been fitted to low-energy π -nucleus scattering and, for comparison purposes, the local Laplacian (LL)¹⁸ and modified Kisslinger (MK)¹⁹ potentials. For all three cases, we have assumed equal neutron and proton mass distributions. For SMC, we have used parameter set I with values interpolated between the $A = 12$ and $A = 16$ cases given there; for both LL and MK, we have used Woods-Saxon matter densities (half-density radius = 2.30 fm, skin thickness = 2.00 fm) with a Coulomb potential for a uniform sphere of charge of radius 3.21 fm. For LL and MK, we have used the πN phase shift parametrization of Salomon.²⁰ He has fitted an analytic function to recent phase shift data²¹ so that the resulting scattering amplitudes are smooth functions of energy from 0-250 MeV. Finally, with the poten-

tial fixed, the resulting Klein-Gordon equation was integrated numerically through use of the program PIRK.²²

In the experiment, targets of adenine ($\text{C}_5\text{H}_5\text{N}_5$) were irradiated with bremsstrahlung of maximum energy 150-700 MeV at the Lund electron synchrotron. The adenine powder was pressed into solid disks of 20 mm diameter and 4 mm thickness. Carbon disks having the same dimensions were used for monitoring. The disks were placed in an uncollimated beam to optimize the photon flux. The ^{14}O daughter nuclei were identified by the 2.31 MeV deexcitation gamma rays, measured by a $35 \text{ cm}^3 \text{ Ge(Li)}$ detector connected to a multi-channel analyzer. The short (70.6 sec) half-life of the product nucleus made it necessary to use a pneumatic system to transport the irradiated samples to the measurement area. With this system, the samples were irradiated and measured within 180 sec, the measurements beginning 20 sec after irradiation. Because of low counting rates, the counts from several runs (as many as 30 at low energies) were accumulated at each end-point energy. The monitor reaction²³ $^{12}\text{C}(\gamma, n)^{11}\text{C}$ was used to obtain absolute yields (cross section per equivalent quantum). In Fig. 1 we have plotted yields as a function of maximum energy. At 150 MeV (5.3 MeV over threshold) no activity was observed from ^{14}O above the background level. The error bars in the figure are statistical with total systematic error estimated to be $\pm 15\%$ [this figure does not include contributions from the $(\gamma, 2n)$ and (p, n) reactions discussed below]. Yields from the reaction²⁷ $^{12}\text{C}(\gamma, \pi^-)^{12}\text{N}$ are shown for comparison.

The residual nucleus ^{14}O can also be produced

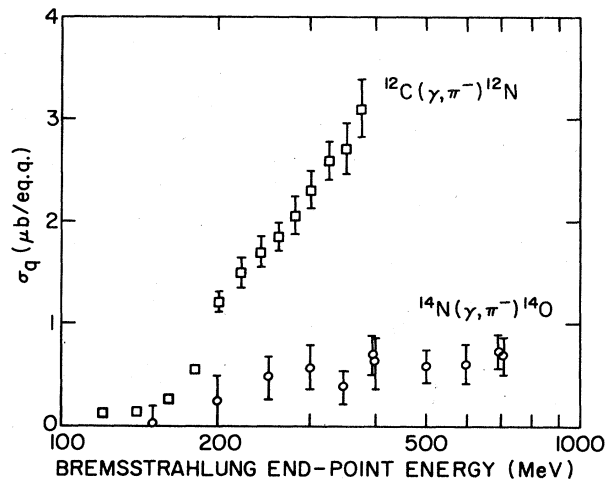


FIG. 1. Bremsstrahlung cross section per equivalent quantum, σ_q , vs. end-point energy. The ^{12}C results are taken from Ref. 27.

by the $(\gamma, 2n)$ reaction on oxygen impurities in the samples. The H_2O content in the samples was 0.25% as given by the manufacturer.²⁴ From the recently measured $^{16}O(\gamma, 2n)^{14}O$ yield curve,²⁵ the contribution to the photopion yield could be determined. It was found to be $0.05 \mu\text{b}/\text{eq.q.}$ at 150 MeV, rising gradually to $0.10 \mu\text{b}/\text{eq.q.}$ at $E_\gamma \geq 400$ MeV. Another possible background contribution arises from photoprotons produced in the adenine targets. The same final nucleus can then be produced via the reaction $^{14}N(p, n)^{14}O$. This background was difficult to determine in the present experiment since the statistical errors in the measurements are large. The results of similar studies,^{26, 27} on ^{12}C indicate that this two-step process is not important here. No corrections were carried out for the two background contributions, since, taken together, they are half as large as the statistical errors in the experimental points.

From the experimental yield points in Fig. 1, the cross section was deduced by the photon difference method together with the smoothing procedure described in Ref. 28. The large errors in the yield data made it necessary to apply strong smoothing to avoid oscillations in the cross section. The final cross sections with error are shown by the shaded areas in Figs. 2, 3, 4, 5, and

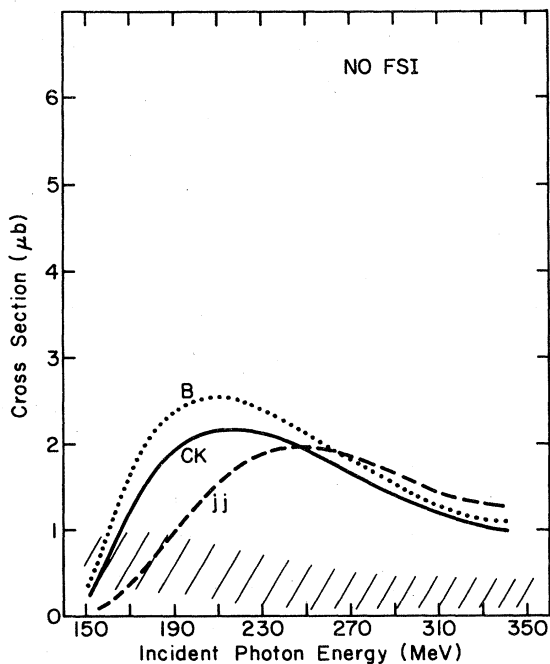


FIG. 2. Total cross section versus incident photon energy for the case $V_{\text{opt}} = 0$. Wave functions are (a) jj coupling (jj); (b) Baer *et al.* (Ref. 4); (B); (c) Cohen-Kurath (Ref. 14) (CK). Present experimental results are denoted by crosshatched area.

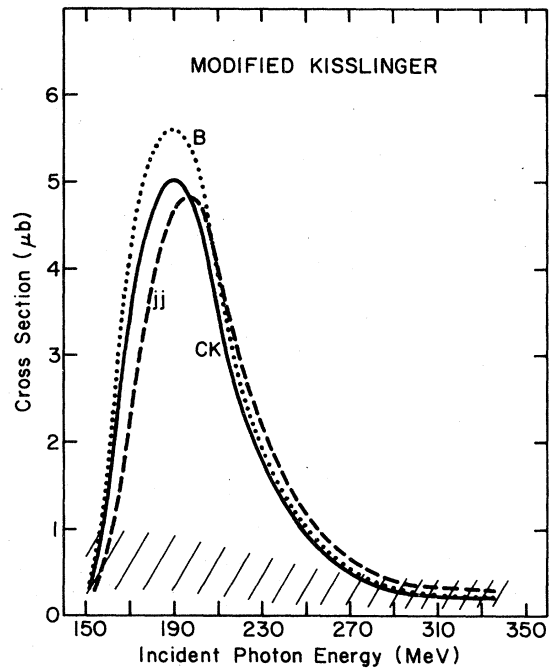


FIG. 3. Same as Fig. 2 for $V_{\text{opt}} =$ modified Kisslinger potential (Ref. 19).

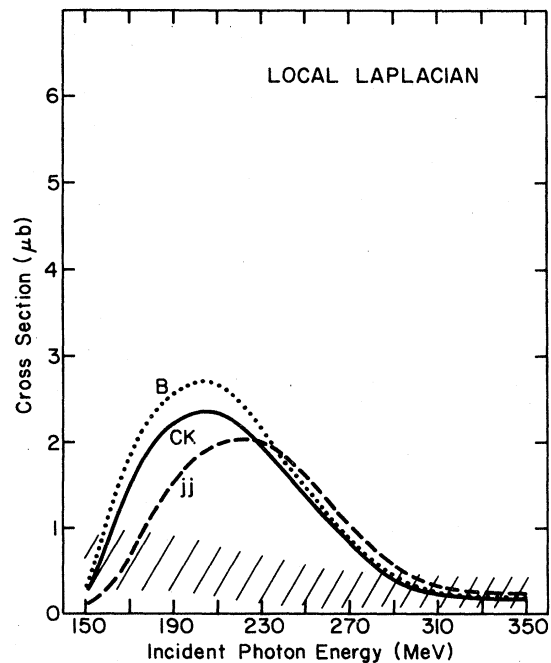


FIG. 4. Same as Fig. 2 for $V_{\text{opt}} =$ local Laplacian potential (Ref. 18).

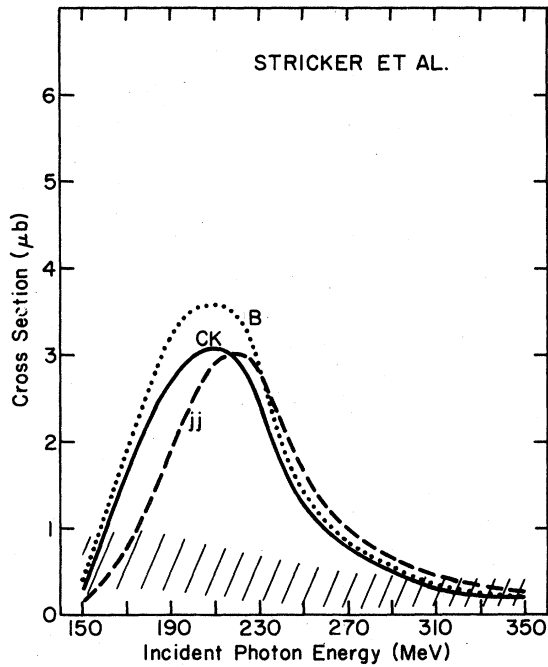


FIG. 5. Same as Fig. 2 for V_{opt} = potential of Stricker *et al.* (Ref. 17).

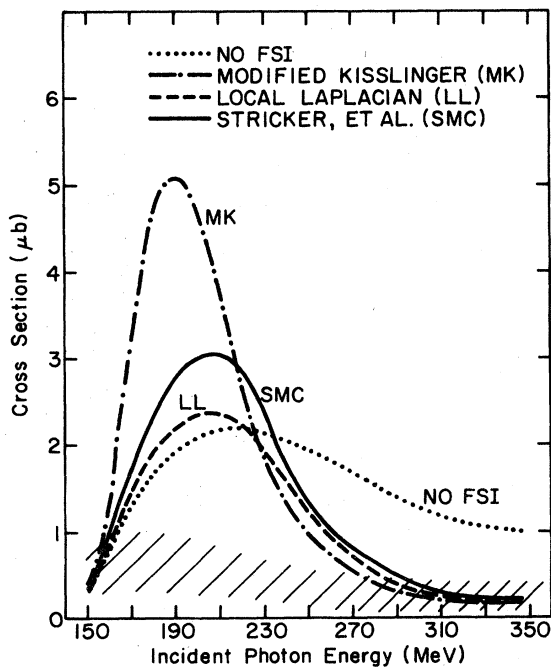


FIG. 6. Total cross section versus photon energy for Cohen-Kurath wave functions and a variety of optical potentials. Present experimental results are denoted by cross-hatched area.

6. It is interesting to compare the magnitude of the cross section to that²⁷ of $^{12}\text{C}(\gamma, \pi^-)^{12}\text{N}(\text{g.s.})$ (Fig. 1). Although there is strong disagreement with the Bates result²⁶ in the threshold region, the ^{12}C cross sections in the energy region 200–400 MeV²⁷ are approximately 5 times larger than those for the ^{14}N reactions.

In Fig. 7, we plot, for jj and CK wave functions and all choices of final state interactions, the difference $\sigma_{\text{av}} - \sigma$, where σ is the cross section calculated using Eq. (1) and σ_{av} is the axial vector contribution to σ . Near threshold, this quantity is relatively independent of both nuclear wave function and optical potential. For all combinations except $jj + \text{MK}$, linear increases are found from zero at threshold (144.7 MeV) to $0.14 \pm 0.06 \mu\text{b}$ at $E_\gamma = 155 \text{ MeV}$; in the case of $jj + \text{MK}$, significantly less damping of the pion momentum dependent contributions occurs so that interference between σ_{av} and $\sigma_{\text{non-av}}$ is less complete (cf. Figs. 3 and 6).

Figures 2–5 illustrate the dependence of the cross sections upon nuclear wave function for fixed optical potential. We note first of all that, consistent with expectation and experiment, cross sections in the near threshold region are consid-

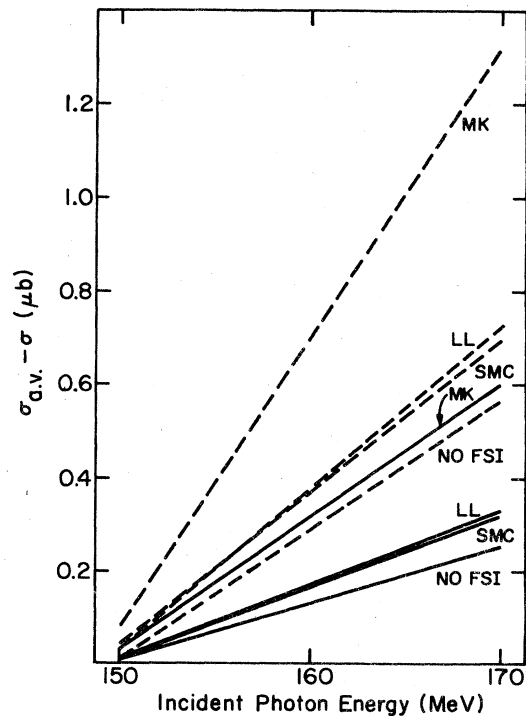


FIG. 7. Pion momentum dependent contributions to the total cross section σ . σ_{av} is the axial vector contribution. Dashed lines are for jj and solid lines for CK wave functions. Optical potentials are from Ref. 17 (SMC), Ref. 18 (LL), and Ref. 19 (MK). Threshold is 144.7 MeV.

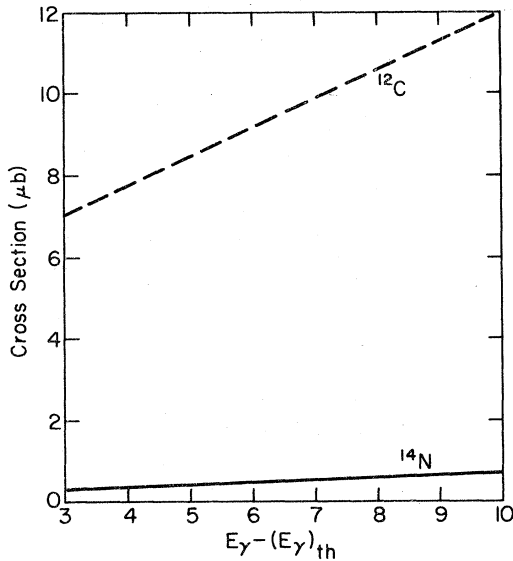


FIG. 8. Total cross section as a function of photon energy over threshold for the near threshold region. The calculations are for (Ref. 29) $^{12}\text{C}(\gamma, \pi^-)^{12}\text{N}$ and $^{14}\text{N}(\gamma, \pi^-)^{14}\text{O}$. Wave functions are Cohen-Kurath (Ref. 14); $V_{\text{opt}} = 0$.

erably smaller than for $^{12}\text{C}(\gamma, \pi^-)^{26,27}$ for all three sets of wave functions. Calculations similar to these, carried out on $A = 12$, lead to results²⁹ 15–30 times greater in the region 3–10 MeV over threshold. This feature is illustrated in Fig. 8 for CK wave functions and no final state interactions. In the energy range 220–450 MeV, the ^{12}C and ^{14}N results are essentially identical for all optical potentials. We note, secondly, that the results for the two “realistic” wave functions are in all cases quite similar with peak locations closer to experiment than for the jj wave functions. In the “post-resonance” region this disparity tends to decrease with energy so that for $E_\gamma \geq 230$ MeV the predictions differ by only a few percent for any final state interaction. Closer to threshold, the CK and jj wave functions also yield similar cross sections but in this region the near vanishing of the GT matrix element for CK wave functions might have led one to expect a far

smaller cross section than for the jj wave functions. That this does not occur is due to the dominant role played by the quadrupole component $[\sigma \otimes Y_2]^{(1)}$ of the photoproduction matrix element.^{9,10} Inspection of this matrix element, $\langle ^{14}\text{O} || j_1(\text{qr}) [\sigma \otimes Y_1]^{(1)} || ^{14}\text{N} \rangle$, indicates that both the $l=0$ and $l=2$ components of the multipole decomposition of $e^{i\mathbf{q}\cdot\mathbf{r}}$ (q = momentum transfer) contribute to the cross section (we ignore final state effects for ease of discussion). In standard notation, the former is proportional to $(C_s^{01} C_s^{10} - (1/\sqrt{3}) C_p^{01} C_p^{10})$, the latter to $(\sqrt{12} C_s^{01} C_D^{10} + \sqrt{5} C_p^{01} C_p^{10} + \sqrt{27/2} C_p^{01} C_D^{10})$. Inserting numbers, we find the s -wave ratio $\sigma(\text{CK})/\sigma(jj)|_s = 2.03 \times 10^{-6}$ consistent with predictions for GT rates. We also find $\sigma(\text{CK})/\sigma(jj)|_d = 0.92$. The CK cross sections are completely dominated by the quadrupole term while both s and d states make sizable contributions to $\sigma(jj)$.

The final point we make is that although all combinations of wave function and optical potential lead to agreement with experiment in the near threshold region and for $E_\gamma \geq 270$ MeV, the results in the vicinity of the resonance are uniformly high. It is interesting to note how sensitive are the predictions in the resonance region to the assumed form of V_{opt} (Fig. 6). In particular, the marked difference between the MK predictions on the one hand and the LL and SMC on the other gives added weight to the observation^{10,30} that optical potentials containing $\nabla \cdot \nabla \rho$ terms may induce unrealistically high momentum components into the pion wave function which can distort production processes which peak in the surface region of the nucleus. These effects are currently under investigation.³¹ What is apparent from the results of this calculation is that the sensitivity of charged pion photoproduction to details of the low energy optical potential can be used to provide valuable information on the π -nucleus interaction in the region in which it is most poorly defined.

One of us (N.F.) would like to thank Dr. Nils Robert Nilsson and NORDITA for supporting his visits to Lund. One of us (V. DeC.) would like to thank Dr. M. Singham for the 80 MeV SMC parameters and for discussing with him his work on $^{14}\text{N}(\gamma, \pi^-)$ with F. Tabakin.³²

¹F. A. Ajzenberg and T. Lauritsen, *Rev. Mod. Phys.* **24**, 321 (1952).

²G. S. Sidhu and J. B. Gerhart, *Phys. Rev.* **148**, 1024 (1966).

³M. Ericson and M. Rho, *Phys. Rep.* **5**, 58 (1972).

⁴Helmut W. Baer *et al.*, *Phys. Rev. C* **12**, 921 (1975).

⁵C. Tzara, in *Proceedings of the International Topical Conference on Meson-Nuclear Physics*, Pittsburgh,

edited by P. D. Barnes, R. A. Eisenstein, and L. S. Kisslinger (AIP, New York, 1976).

⁶N. C. Mukhopadhyay, *Phys. Lett.* **44B**, 33 (1973).

⁷J. H. Koch and T. W. Donnelly, *Nucl. Phys.* **B64**, 478 (1973).

⁸G. N. Epstein, M. K. Singham, and F. Tabakin, *Phys. Rev. C* **17**, 702 (1978).

⁹N. Freed and P. Ostrander, *Phys. Lett.* **61B**, 449 (1976).

- ¹⁰I. Blomqvist *et al.*, Phys. Rev. C 15, 988 (1977).
¹¹M. L. Goldberger and K. M. Watson, *Collision Theory* (Wiley, New York, 1964).
¹²F. A. Berends, A. Donnachie, and D. L. Weaver, Nucl. Phys. B4, 54 (1967); B4, 103 (1967).
¹³D. L. Weaver, Phys. Lett. 26B, 451 (1968).
¹⁴S. Cohen and D. Kurath, Nucl. Phys. 73, 1 (1965); H. J. Rose, O. Häusser, and E. K. Warburton, Rev. Mod. Phys. 40, 591 (1968).
¹⁵S. Y. Lee, Ph.D. dissertation, SUNY at Stony Brook, 1972 (unpublished).
¹⁶S. Lie, Nucl. Phys. A181, 517 (1972).
¹⁷K. Stricker, H. McManus, and J. A. Carr, Phys. Rev. C 19, 929 (1979).
¹⁸H. K. Lee and H. McManus, Nucl. Phys. A167, 257 (1971).
¹⁹G. A. Miller, Phys. Rev. C 10, 1242 (1974).
²⁰M. Salomon, TRIUMF Report TRI-74-2, Low Energy (0-250 MeV) Pion-Nucleon Phase Shift Fits (1974).
²¹S. Almeded and C. Lovelace, CERN Report TH 1408 (1971); P. W. Coulter, Phys. Rev. Lett. 29, 450 (1972); J. R. Carter, D. V. Bugg, and A. A. Carter, Nucl. Phys. B58, 378 (1973).
²²R. A. Eisenstein and G. A. Miller, Computer Phys. Commun. 8, 130 (1974).
²³G. Hyltén, Nucl. Phys. A158, 225 (1970).
²⁴E. M. Merck AG, Darmstadt.
²⁵B. Johnsson, M. Nilsson, and K. Lindgren, Nucl. Phys. A278, 365 (1977).
²⁶A. M. Bernstein *et al.*, Phys. Rev. Lett. 37, 819 (1976).
²⁷V. D. Epaneshnikov, V. M. Kuznetsov, and O. I. Stukov, Yad. Fiz. 19, 483 (1974) [Sov. J. Nucl. Phys. 19, 242 (1974)].
²⁸K. Tesch, Nucl. Instrum. Methods 95, 245 (1971).
²⁹N. Freed *et al.* (unpublished).
³⁰G. A. Miller and S. C. Phatak, Phys. Lett. 51B, 129 (1974).
³¹N. Freed, P. Ostrander, and K. Srinivasa Rao (unpublished).
³²M. K. Singham and F. Tabakin (unpublished).